

RESEARCH ARTICLE

Open Access



Sensitivity of slip distribution on tsunami trace heights and geological evidences: a case study of the 2011 Tohoku-Oki earthquake

Satoshi Kusumoto^{1*} , Kentaro Imai¹, Takane Hori¹, Daisuke Sugawara² and Kenji Satake³

Abstract

We examined whether it is possible to estimate the tsunami source model of the 2011 Tohoku-Oki earthquake from a comparison of numerical simulations of tsunami propagation and sediment transport, the measured trace heights, and the sediment thickness of tsunami deposits. Twelve models with different subfault numbers were prepared based on a reference model inferred from tsunami waveform inversion. The reference model with 55 subfaults considering rupture propagation and the model with instantaneous slip successfully reproduced both the tsunami trace heights and sediment thickness distribution of tsunami deposits in the Idagawa Lowland and Sendai Plain. Other models with the same moment magnitude but fewer subfaults could not reproduce the observed trace heights, and the reproducibility of sediment thickness distribution strongly depended on the slip distribution. Models with increased slip amounts and moment magnitude could reproduce the trace heights; however, the simulated sediment thickness was underestimated for the Idagawa Lowland while overestimated for the Sendai Plain. Our results indicate that the combination of trace heights, sediment thickness of tsunami deposits, and numerical simulations of tsunami propagation and sediment transport can be used to estimate historical earthquakes and tsunamis. Efforts should be made to increase the number of subfaults for the study of historical events, although the obtained solutions may not be unique because of fewer trace heights or tsunami deposit data.

Keywords 2011 Tohoku-Oki tsunami, Tsunami deposits, Sediment transport numerical simulation

1 Introduction

At 05:46:18.1 UTC, March 11, the 2011 Tohoku earthquake (Mw 9.0) occurred as the largest earthquake in Japanese instrumental observation history. It triggered large tsunami that caused enormous damage to the Pacific coast of the Tohoku region of northeastern Japan, including 19,765 fatalities, 6242 reported

injuries, and 2553 people reported missing (according to the Fire and Disaster Management Agency, as of March 1, 2023). The seismic waves, crustal deformation, and tsunami were recorded by the Global Seismographic Network, GNSS Earth Observation NETWORK system, and Deep-ocean Assessment and Reporting of Tsunamis, respectively. The initial source models of the 2011 Tohoku-Oki earthquake have been proposed from instrumental observations (e.g., Ide et al. 2011; Ozawa et al. 2011; Satake et al. 2013). These models have the following common features: There was a large slip area off the coast of Miyagi Prefecture, with a maximum slip amount of 30–70 m, and the duration of fault rupture was approximately 3–5 min. After the earthquake and tsunami, tsunami surveys were conducted by joint research groups with the participation of 299 tsunami

*Correspondence:

Satoshi Kusumoto
kusumotos@jamstec.go.jp

¹ Japan Agency for Marine–Earth Science and Technology, 3173–25 Showa-machi, Kanazawa, Yokohama 236-0001, Japan

² International Research Institute of Disaster Science, Tohoku University, 468-1 Aoba, Aramaki, Aoba-Ku, Sendai, Miyagi, Japan

³ Earthquake Research Institute, University of Tokyo, 1-1-1, Yayoi, Bunkyo-ku, Tokyo 113-0032, Japan



© The Author(s) 2023. **Open Access** This article is licensed under a Creative Commons Attribution 4.0 International License, which permits use, sharing, adaptation, distribution and reproduction in any medium or format, as long as you give appropriate credit to the original author(s) and the source, provide a link to the Creative Commons licence, and indicate if changes were made. The images or other third party material in this article are included in the article's Creative Commons licence, unless indicated otherwise in a credit line to the material. If material is not included in the article's Creative Commons licence and your intended use is not permitted by statutory regulation or exceeds the permitted use, you will need to obtain permission directly from the copyright holder. To view a copy of this licence, visit <http://creativecommons.org/licenses/by/4.0/>.

researchers, such as coastal engineers, seismologists, and geologists from 64 universities and institutes throughout Japan. As of December 29, 2012, a total of 5907 tsunami trace heights have been reported from the Pacific coast of Hokkaido to Kagoshima Prefecture (Fig. 1, Mori et al. 2011).

The tsunami associated with this earthquake left tsunami deposits in the coastal lowlands along the Pacific coast of the Tohoku region. Thickness, sedimentological structure, and grain size distribution of the deposit have been carefully investigated and summarized by tsunami deposit researchers (e.g., Goto et al. 2011; Kusumoto et al. 2018). The sediment thickness and grain size of tsunami deposits vary greatly depending on the survey site, and they are closely related to the tsunami source and topography/bathymetry (e.g., Goto et al. 2014). Coastal vegetation also affects the character of tsunami deposits. For example, Kusumoto et al. (2020) quantitatively evaluated changes in deposition volume of tsunami deposits in areas with/without coastal forest. In addition, the research on tsunami-induced sediment transport has progressed greatly since the 2011 Tohoku-Oki event. Tsunami hydraulic experiments have been performed to establish transport formula for fine- to medium-grained sands (e.g., Takahashi et al. 2011), and large-scale calculations using a supercomputer have enabled the simulation of tsunami sediment transport in regional scale (e.g.,

Yamashita et al. 2016). The numerical simulation of tsunami sediment transport can be now utilized to study past tsunami events (e.g., Sugawara et al. 2019).

To forecast characteristics of future megathrust earthquakes occurring in subduction zones, it is important to know how far the fault rupture extended or how much strain energy was released during past events. However, it is difficult to estimate the magnitude of past tsunamis because it is often impossible to measure the run-up heights or distances and exact localities of the observation at the time of the tsunami attack, especially for events that occurred before instrumental observation. For those events, historical documents and geological evidence are exclusive records. Therefore, a technique for estimating the source of historical tsunami events from such non-instrumental tsunami records is needed. In this study, we examined whether it is possible to estimate the initial tsunami source model from comparisons of numerical simulations of tsunami propagation and tsunami sediment transport, tsunami trace heights, and sediment thickness distribution of tsunami deposits for the 2011 Tohoku-Oki earthquake. The 2011 event provides a valuable modern analog to validate the proposed method because the tsunami source has been estimated from instrumental records, and tsunami data such as trace heights and deposits are also available.

2 Data and methods

2.1 Documental records

Among the tsunami trace points surveyed by the Tohoku Earthquake Tsunami Joint Survey Group, 2364 tsunami inundation heights with the highest reliability (i.e., reliability rank A) are located in the range of 35° to 41° N. Imai et al. (2013) have investigated the dependence of alongshore distribution of tsunami trace data for tsunami source estimation and concluded that deviation from an optimal solution can be minimized if the alongshore data distribution is approximately the same as the size of the tsunami source, and the tsunami data are obtained at intervals of about 5% with respect to the size of the tsunami source. In this study, the tsunami data are averaged at 0.1° intervals (approximately 5% for fault length; Imai et al. 2013), yielding 60 ranges (Figs. 1 and 2).

2.2 Geological records

Numerical simulation of tsunami sediment transport is expected to reproduce the depositional process for a simple topography with few artificial structures. We chose three sites from previous researches on tsunami deposits with different topography: a reclaimed lagoon (Idagawa Lowland, Minami-soma City, Fukushima Prefecture; Kusumoto et al. 2018), an alluvial plain (Sendai Plain, Sendai City, Miyagi Prefecture; Abe et al. 2012), and a

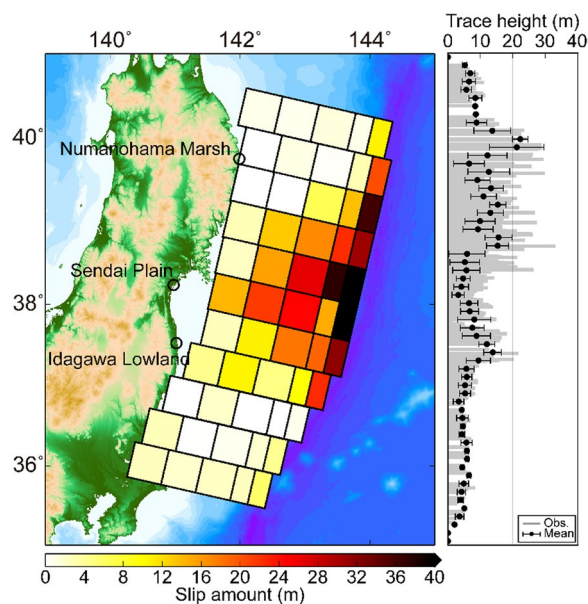


Fig. 1 Final slip distribution of the 2011 Tohoku-Oki earthquake (Satake et al. 2013) and spatial distribution of tsunami trace heights (Mori et al. 2011). Gray bars, black dots, and error bars show the observations, mean, and standard deviation averaged at 0.1° intervals, respectively

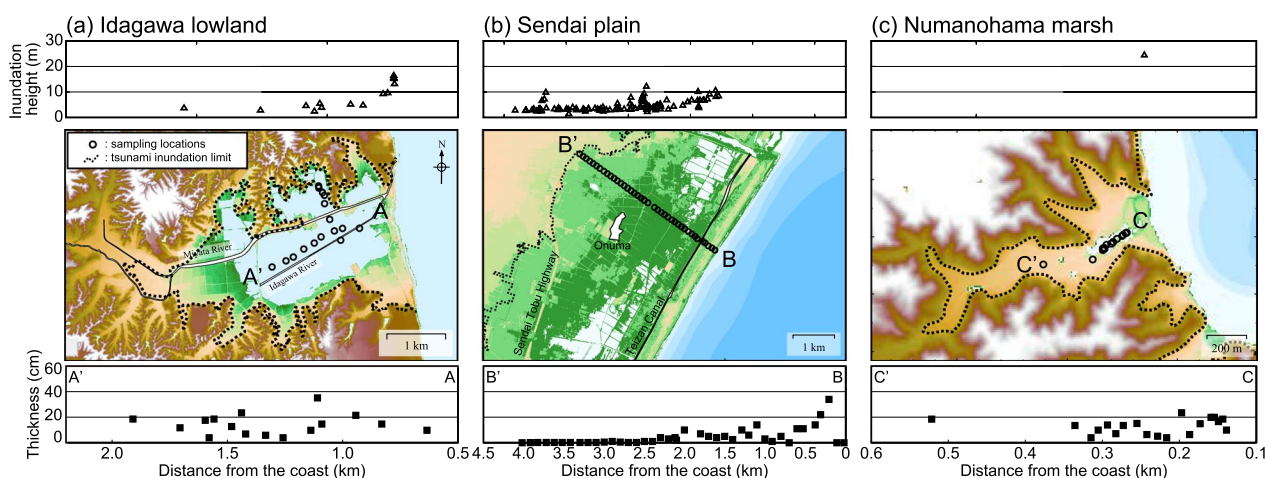


Fig. 2 Tsunami trace heights (upper panels), topography (middle panels), and the observed sediment thickness (lower panels) of the 2011 Tohoku-Oki tsunami deposits along each transect. **a** Idagawa Lowland, Fukushima Prefecture; **b** Sendai Plain, Miyagi Prefecture; and **c** Numanohama Marsh, Iwate Prefecture, Japan. Circles on the map indicate sampling locations, and the dotted curves show the limits of the tsunami inundation

wetland in a V-shaped valley (Numanohama Marsh, Miyako City, Iwate Prefecture; Goto et al. 2017) (Figs. 1, 2). Table 1 summarizes the characteristics of the 2011 Tohoku-Oki earthquake tsunami deposits at each survey site. The deposits of the Idagawa Lowland and Sendai Plain are mainly composed of medium to coarse sand, while that of the Numanohama Marsh is mostly composed of gravel. The sediment thickness is ~40 cm at all study sites and abruptly becomes thinner with increasing distance from the coast.

2.3 Numerical simulations

Tsunami inundation heights on the Pacific coast of Tohoku were calculated using the high-performance tsunami calculation code JAGURS (Baba et al. 2015, 2017). The two-dimensional nonlinear long-wave equations were solved for the bathymetry and topography of the entire Pacific coast of Tohoku. The topographic and bathymetric grid interval was set at 2 arcsec (Chikasada 2020), without using a nesting grid, and the computational time was 3 h from the occurrence of the earthquake. The computational time interval was set at 0.1 s to satisfy the Courant–Friedrichs–Lewy (CFL) condition.

For numerical simulation of tsunami sediment transport, an existing code (TUNAMI-STM; Yamashita et al. 2016), which consists of the two-dimensional nonlinear long-wave equations, and the advection equation of suspended load and continuity equations for bedload and suspended load layers (e.g., Takahashi et al. 1999, 2011), was adopted. Sand particles were mostly transported in suspension; therefore, the sediment deposition and erosion were closely related to flow velocity of a tsunami. An increase in flow velocity eroded the basement, and a decrease in flow velocity caused sand depositions.

Topographic and bathymetric data were resampled from 450 to 5.56 m for the nested grids based on the M7000 series (about 20 m grid intervals) and the digital elevation model (5 m grid intervals) published by the Geospatial Information Authority of Japan. The computational time was set to 3 h from the occurrence of the earthquake, and the computational time interval was set to 0.1 s to satisfy the CFL condition.

Saturation concentration, which gives variable limits to pickup rate of the suspended load, is considered using the turbulence energy balance model (e.g., Yamashita et al. 2016; Sugawara et al. 2019). The mean grain size was set to 0.267 mm at all survey sites, and

Table 1 The 2011 Tohoku-Oki tsunami deposits

	Number of cores	Grain size	Sediment thickness (cm)	Maximum inundation distance from coast (m)
Idagawa Lowland	16	Medium to coarse sand	4–36	1920
Sendai Plain	41	Medium to coarse sand	~34	4020
Numanohama Marsh	20	Pebbles	4–23	990

the grain size-dependent parameters (i.e., coefficients for bedload rate (4.0) and pickup rate (4.40×10^{-5}), settling velocity (0.0392 m/s), and critical shear stress (0.0383)) were based on Takahashi et al. (2011) and Gusman et al. (2018).

Coastal forest is distributed along the coastline of the Sendai Plain. The forest affected not only the flow velocity but also sediment transport by the tsunami (e.g., Kusumoto et al. 2020). Therefore, a composite equivalent roughness coefficient to include the tsunami damping effect by the forests (e.g., Aburaya and Imamura 2002; Kusumoto et al. 2020) was adopted in this study. Here, the forest cover and trunk width of the coastal forest were set at 0.39% and 0.13 m, respectively, based on survey results before the 2011 Tohoku-Oki earthquake (e.g., Harada et al. 2000; Imai et al. 2009).

2.4 Tsunami source models

The coseismic seafloor displacement is calculated from the fault parameters of the tsunami source model of the 2011 Tohoku earthquake, which was estimated from a comparison of the simulated and observed waveforms at wave gauge stations near Japan (Okada 1985; Tanioka and Satake 1996; Satake et al. 2013). The Kajiura filter (Kajiura 1963) is applied to calculate the initial sea surface displacement from the coseismic seafloor displacement.

The 55-subfault model with the delayed slip was set as a reference model (Model 1). Based on the reference model, other 11 models (Models 2–12) were prepared (Fig. 3, Table 2). The fault ruptures in Models 3 and 4 extended only to the deep and shallow parts of the plate interface, respectively. Models 5–12 had different numbers of subfaults. In Models 5–9, the slip amounts of each subfault were averaged from Model 1. In Models 9–12, the average slip amount was multiplied by 1.9,

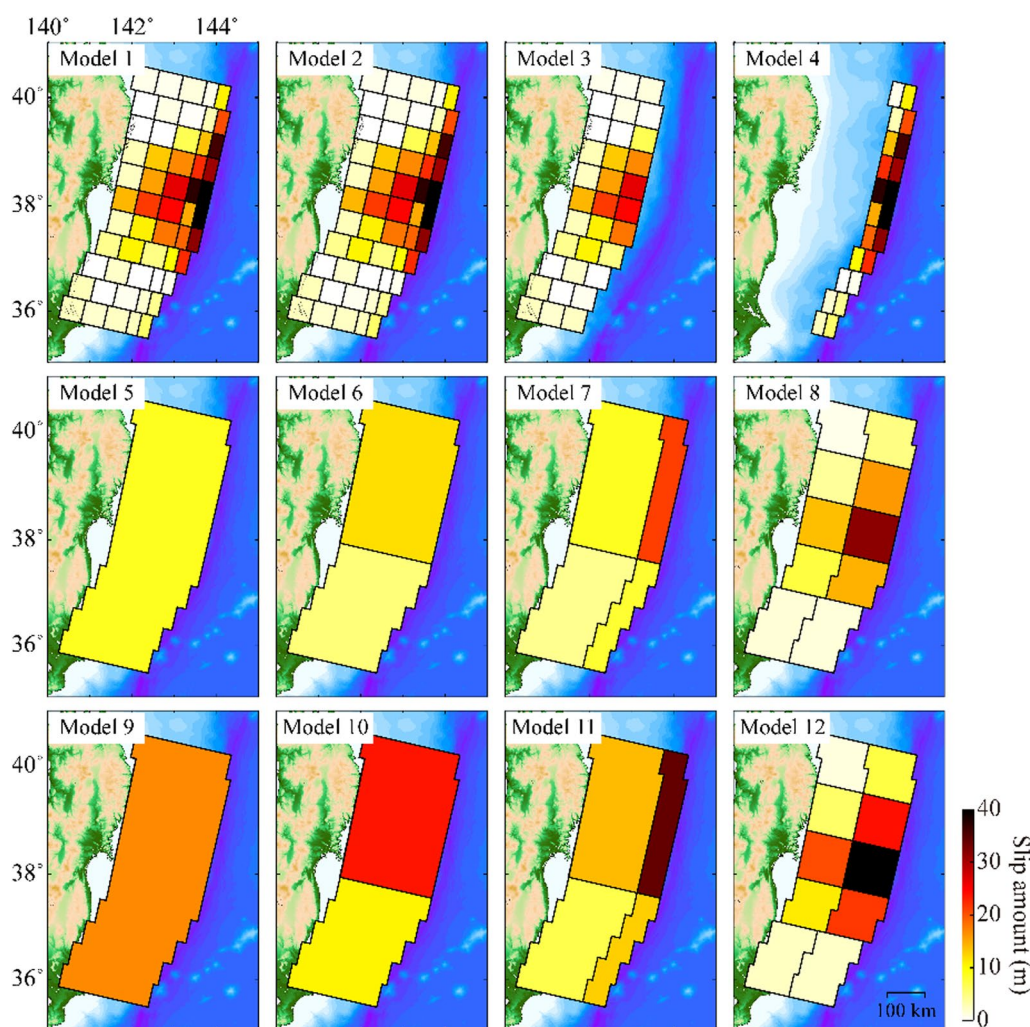


Fig. 3 The initial tsunami source models examined in this study. All models are based on the 55-subfault reference model (Satake et al. 2013)

Table 2 The initial tsunami source models in this study

Model	Mw	Fault rupture	Number of subfaults	Slip distribution	Range of slip amount (average) (m)
1	9.0	Propagating slip	55	Variable	0–69 (9.5)
2	9.0	Simultaneous	55	Variable	0–69 (9.5)
3	8.8	Simultaneous	33	Variable	0–26 (18.6)
4	8.8	Simultaneous	22	Variable	0–69 (6.4)
5	9.0	Simultaneous	1	Uniform	9.5 (9.5)
6	9.0	Simultaneous	2	Variable	7.1–11.9 (9.5)
7	9.0	Simultaneous	4	Variable	4.4–21.3 (9.5)
8	9.0	Simultaneous	10	Variable	0.9–31.7 (9.5)
9	9.1	Simultaneous	1	Uniform	18.1 (18.1)
10	9.1	Simultaneous	2	Variable	14.2–23.7 (19.0)
11	9.1	Simultaneous	4	Variable	7.0–34.1 (15.2)
12	9.1	Simultaneous	10	Variable	1.3–47.6 (14.3)

2.0, 1.6, and 1.5, respectively, so that the tsunami trace height could be reproduced by the calculated tsunami height of Models 5–8. Because distribution and thickness of tsunami deposits are controlled by flow velocity, these models do not necessarily reproduce the tsunami deposits. The rise time was set at 300 s with variable start times of rupture on each subfault in Model 1, and in the other models, it was set at 30 s (Satake et al. 2013). The reproducibility of the simulation was evaluated by the geometric mean and standard deviation (K and κ ; Aida 1978). The simulations match with the observations when the geometric mean or standard deviation is close to 1, an overestimation if the geometric mean is less than 1, and an underestimation if it is greater than 1.

3 Results and discussion

3.1 Trace heights

Figure 4 illustrates a comparison of observed tsunami trace heights and the simulated heights for each model. The simulated heights from Model 1 well match the observations. Although Model 2 cannot explain the maximum trace heights around 40° N, 37.5° N, and 36° N, the simulated heights are roughly consistent with observations at the other locations. The difference between Models 1 and 2 is attributed to the effects of rupture propagation which is represented by rise time of 30–300 s and variable start times of rupture. Both Models 3 and 4 underestimated the observations, indicating that the rupture should cover both shallow and deep segments at the plate boundary to explain the tsunami trace

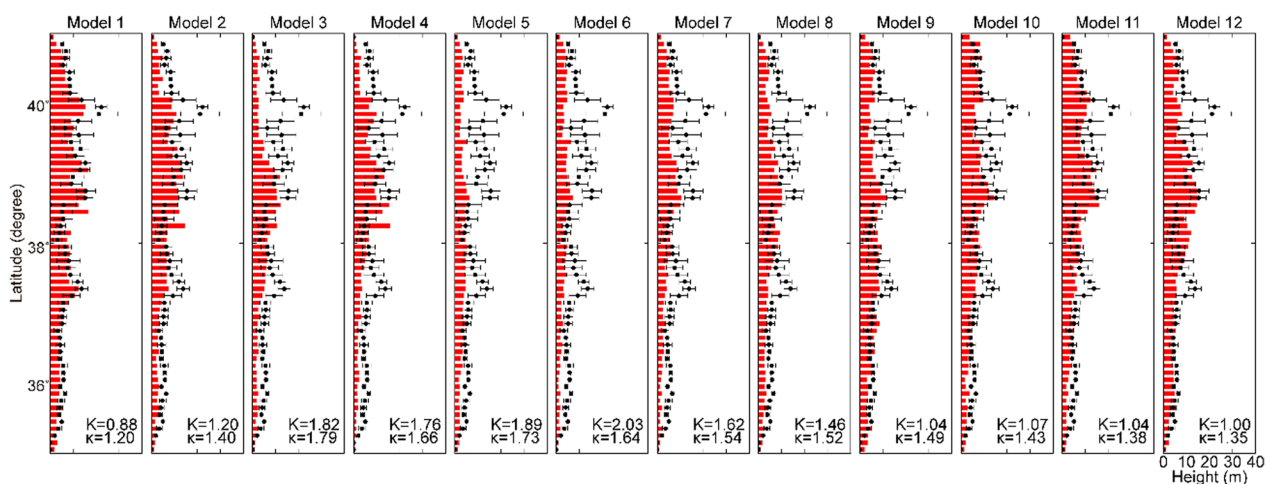


Fig. 4 Comparison of the observed tsunami trace heights (mean: black dots, standard deviation: error bars) and the simulated heights (red bars). K and κ show the geometric mean and standard deviation of Aida (1978), respectively

heights, in addition to the fact that these models have smaller overall seismic moment. The comparison of the simulated results from Models 5–8 shows that the reproducibility is low with a smaller number of subfaults. The geometric means of Models 9–12 are close to 1, but the standard deviations range from 1.35 to 1.49, indicating high variability compared with Model 1.

Additional file 1: Figure S1 shows a comparison of observed tsunami inundation heights and the simulated heights for each model around the Idagawa Lowland and Sendai Plain. For the Idagawa lowland, Model 2 underestimated the tsunami inundation height near the coastline, compared to Model 1. Conversely, Model 2 overestimated the heights for Sendai Plain. This can also be attributed to the difference in fault rupture propagation.

3.2 Sediment thickness of tsunami deposits

Figure 5 shows the comparisons of the observed and simulated sediment thickness at the three sites (Fig. 2). The 2011 Tohoku-Oki tsunami deposits in the Idagawa Lowland were characterized by being thin in the center of the lowland (approximately 1.2–1.4 km from the coast) and being thick at both sides (~1.0 km and ~1.5 km) (Fig. 2, Kusumoto et al. 2018). The simulated sediment thickness mostly produced mountain-shaped distribution with a peak at around 1.5 km from the coast, and the above observed feature (thin in the center) could not be reproduced. Model 2 had the geometric mean closest to 1, followed by Model 1. Models 4, 6, 7, and 8 showed a characteristic trend of landward thinning of sediment. In these models, sediments were not transported into the lowland, probably because of smaller slip amounts in the southern fault area. The result of Models 9–12 indicates that a large slip is required in the southern part of the tsunami source for sediment to be transported inland. The geometric means of Models 9–12 approached 1 when the average slip amount was increased, but they were still greater than 1, indicating underestimation on average.

The 2011 Tohoku-Oki tsunami deposits on the Sendai Plain were characterized by being thickest near the coastline and thinning rapidly with distance from the coast (Fig. 2, 5b). The simulated sediment thickness in Models 1 and 2 well matched the observations. Model 4, which only ruptured the subfaults near the trench axis, produced the deposition only about 1 km from the coast; therefore, it is not suitable as an initial tsunami wave source from a viewpoint of sediment thickness of tsunami deposits. Among the models with a smaller number of subfaults (Models 5–8), the geometric mean was closest to 1 for Model 8. The reproductivity may depend strongly on wavelength of the tsunami. The tsunami generated by Model 7 is dominated by short wavelengths, so the inundation area is limited to the coastline and

sediment movement is also limited. Conversely, the tsunami generated by Model 8 has a relatively long wavelength. Therefore, the tsunami-inundated deep inland and simulated sediment thickness match the observations. The geometric means of Models 9–12 were all less than 1, indicating that the simulated results overestimated the observations. This result is opposite to that for the Idagawa Lowland, suggesting that the sediment thickness distribution of tsunami deposits strongly depends on the topography of the survey site.

The 2011 Tohoku-Oki tsunami deposits of the Numanohama Marsh were about 20 cm thick up to 0.6 km from the coast. This feature cannot be explained by the simulated results, although Model 2 produces sediment transportation into the land. This is because the tsunami deposits were composed mostly of gravels, and the calculation formula for suspended load and bedload layers adopted in TUNAMI-STM may not be applicable to gravels.

3.3 Combination of trace heights and tsunami deposits

Table 3 summarizes the results presented in Sects. 3.1 and 3.2 for the Sendai Plain and the Idagawa Lowland. Models 1 and 2 successfully reproduced both the tsunami trace heights and the sediment thickness distribution of the tsunami deposits. Model 1 considered the slip propagation toward the north based on analyses of tsunami waveforms. However, the trace heights and tsunami deposits contain no information on temporal changes of tsunamis, so the model with instantaneous slip (Model 2) may be more appropriate for estimating the initial tsunami source from trace heights and tsunami deposits. Other models with the same moment magnitude but smaller numbers of subfaults (Models 5–9) could not reproduce the observed trace heights, and the reproducibility of the sediment thickness distribution strongly depended on the slip distribution, as indicated by Models 8 and 11. Models 9–12, which simply increased the slip amounts of Models 5–8 (and the resultant moment magnitude of 9.1), could reproduce the coastal trace heights; however, the simulated sediment thickness was underestimated for the Idagawa Lowland while overestimated for the Sendai Plain.

Finally, we discuss the applicability of the methods to historical tsunami events. Although less information is available for older tsunami events, our finding that a smaller number of subfaults lead to lower reproducibility indicates the importance of adopting subfaults and increasing the number of observed data points, for example, by reexamining historical materials and by conducting tsunami deposit surveys. Rather than simply increasing the amount of slip, it will be necessary to set a large slip area and compare the observations and

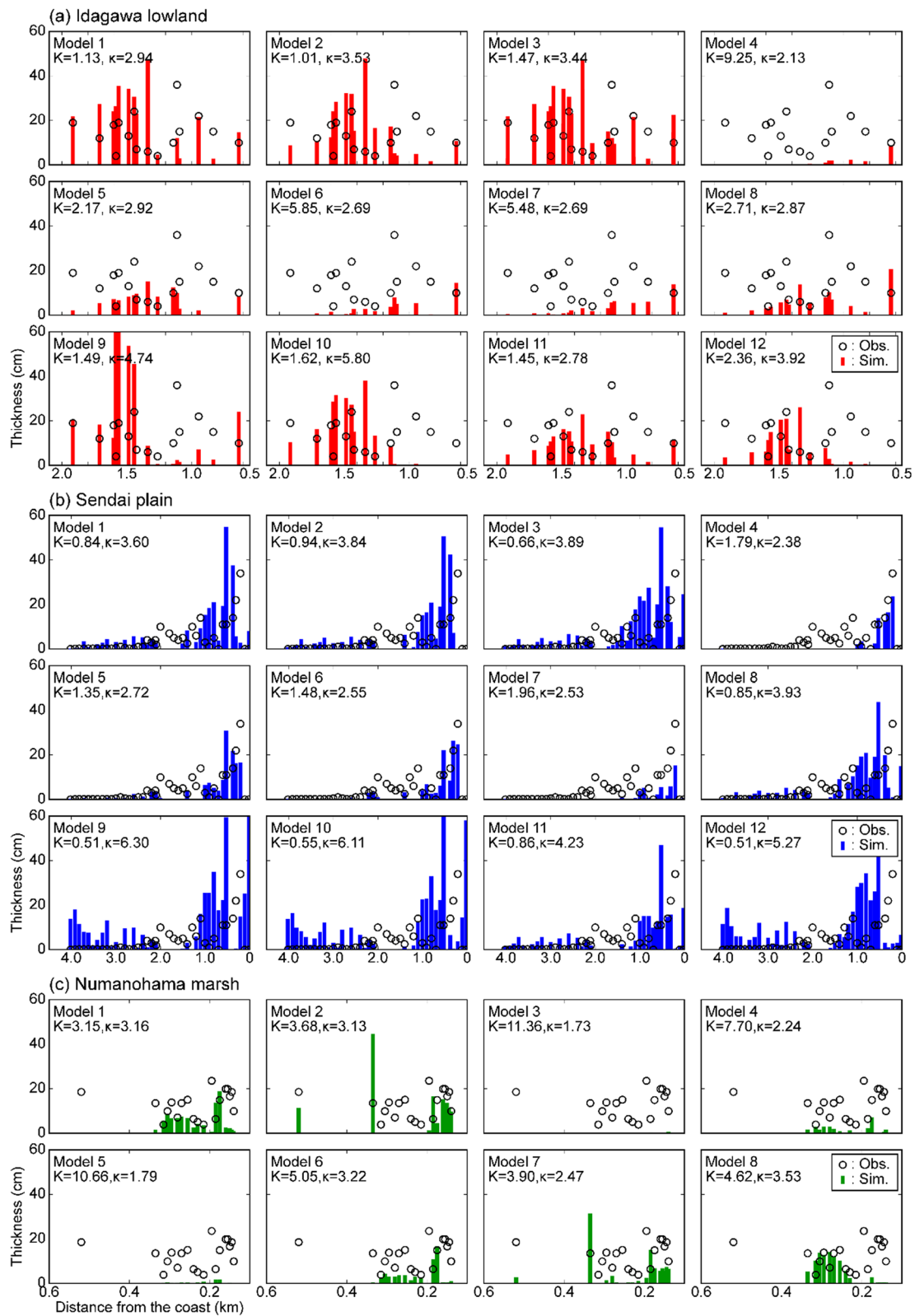


Fig. 5 Comparison of the observed and simulated sediment thickness for 0.267 mm in mean diameter at **a** Idagawa Lowland, **b** Sendai Plain, and **c** Numanohama Marsh

Table 3 Comparison of the geometric means of observed trace heights or tsunami deposits to the simulation results

Model	Mw	Trace heights	Sediment thickness of tsunami deposits	
			Idagawa Lowland	Sendai plain
1	9.0	0.88	1.13	0.84
2	9.0	1.20	1.01	0.94
3	8.8	U 1.82	U 1.47	O 0.66
4	8.8	U 1.76	U 9.25	U 1.79
5	9.0	U 1.89	U 2.17	U 1.35
6	9.0	U 2.03	U 5.85	U 1.48
7	9.0	U 1.62	U 5.48	U 1.96
8	9.0	U 1.46	U 2.71	0.85
9	9.1	1.04	U 1.49	O 0.51
10	9.1	1.07	U 1.62	O 0.55
11	9.1	1.04	U 1.45	0.86
12	9.1	1.00	U 2.36	O 0.51

The symbols (U, O) show that the simulations were underestimated ($K > 1.2$), or were overestimated ($K < 0.8$), where K is the geometric mean (Aida 1978)

numerical simulation results. Gravel-dominant tsunami deposits are outside the applicability of the formulas for suspended sediments and bedload incorporated in TUNAMI-STM. Therefore, the survey sites used for estimating the initial tsunami wave source should be limited to those with sand-dominant tsunami deposits. If a gravel-dominant survey site is used, a formula for the mixed sediment transport of gravels and sand should be used.

4 Conclusions

We examined whether it is possible to estimate an initial tsunami source model for the 2011 Tohoku-Oki event by comparing numerical simulation results for tsunami propagation and sediment transport with measured trace heights and observed sediment thickness of tsunami deposits. Models 1 and 2, based on 55-subfault models obtained by a previous tsunami waveform inversion (Satake et al. 2013), could successfully explain both the tsunami trace heights and the sediment thickness distribution of the tsunami deposits. In other words, the accuracy of the initial tsunami source estimation could be improved by combining numerical simulations of tsunami propagation and sediment transport with tsunami trace heights and sediment thickness of tsunami deposits. The models with fewer subfaults had lower reproducibility, even if the overall moment magnitude was the same. Therefore, it is important to increase the number of subfaults as well as increasing the number of trace points, for example, by reexamining historical materials and conducting tsunami deposit surveys. We conclude

that the combination of trace heights, sediment thickness of tsunami deposits, and numerical simulations of tsunami propagation and sediment transport can be used to estimate historical earthquakes and tsunamis.

Supplementary Information

The online version contains supplementary material available at <https://doi.org/10.1186/s40645-023-00582-y>.

Additional file 1. Figure S1. Comparison of observed tsunami inundation heights and the simulated heights for each model around the Idagawa Lowland and Sendai Plain. Triangles and red/blue bars show the observed trace heights and simulated heights, respectively. K and κ are the geometric mean and standard deviation by Aida (1978).

Acknowledgements

We would like to thank the editor Dr. Takuto Maeda and two anonymous reviewers for providing and valuable comments and suggestions that were helpful for improved the manuscript. This study is based on the first author's PhD thesis submitted to the University of Tokyo (Kusumoto 2021). This study was also supported by the project "Research project for compound disaster mitigation on the great earthquakes and tsunamis around the Nankai trough region" of the Ministry of Education, Culture, Sports, Science and Technology Japan (MEXT).

Author contributions

KI and TH contributed to the interpretation of the data. KS and DS contributed to the interpretation of the results and discussion. All authors read and approved the final manuscript.

Funding

This work was supported by the project "Research project for compound disaster mitigation on the great earthquakes and tsunamis around the Nankai trough region" of the Ministry of Education, Culture, Sports, Science and Technology Japan (MEXT).

Availability of data and materials

The datasets supporting the conclusions of this article are available in the supplementary information of Kusumoto et al. (2020) (available at <https://doi.org/10.1785/0220200068>), Abe et al. (2012) (available at <https://doi.org/10.1016/j.sedgeo.2012.05.004>), and Goto et al. (2017) (available at <https://doi.org/10.1016/j.quaint.2017.05.014>). The Global Tsunami Terrain Model (GtTM) is also available in the supplementary information of Chikasada (2020) (available at <https://doi.org/10.17598/NIED.0021>).

Declarations

Competing interests

The authors declare that they have no competing interests.

Received: 6 April 2023 Accepted: 7 August 2023

Published online: 25 August 2023

References

- Abe T, Goto K, Sugawara D (2012) Relationship between the maximum extent of tsunami sand and the inundation limit of the 2011 Tohoku-oki tsunami on the Sendai Plain, Japan. *Sed Geol* 282:142–150. <https://doi.org/10.1016/j.sedgeo.2012.05.004>
- Aburaya T, Imamura F (2002) Proposal of a tsunami runup simulation using the combined equivalent roughness model. *Proc Coast Eng JSCE* 49:276–280 (in Japanese)
- Aida I (1978) Reliability of a tsunami source model derived from fault parameters. *J Phys Earth* 26(1):57–73

- Baba T, Takahashi N, Kaneda Y, Ando K, Matsuoka D, Kato T (2015) Parallel implementation of dispersive tsunami wave modeling with a nesting algorithm for the 2011 Tohoku tsunami. *Pure Appl Geophys* 172:3455–3472. <https://doi.org/10.1007/s00024-015-1049-2>
- Baba T, Allgeyer S, Hossen J, Cummins PR, Tsushima H, Imai K, Yamashita K, Kato T (2017) Accurate numerical simulation of the far-field tsunami caused by the 2011 Tohoku earthquake, including the effects of Boussinesq dispersion, seawater density stratification, elastic loading, and gravitational potential change. *Ocean Model* 111:46–54. <https://doi.org/10.1016/j.ocemod.2017.01.002>
- Chikasada N (2020) Global digital elevation model for tsunami inundation calculation. <https://kiyuu.bosai.go.jp/GtTM/>
- Goto K, Chagué-Goff C, Fujino S, Goff J, Jaffe B, Nishimura Y, Richmond B, Sugawara D, Szczuciński W, Tappin DR, Witter R, Yulianto E (2011) New insights of tsunami hazard from the 2011 Tohoku-Oki event. *Mar Geol* 290:46–50. <https://doi.org/10.1016/j.margeo.2011.10.004>
- Goto K, Hashimoto K, Sugawara D, Yanagisawa H, Abe T (2014) Spatial thickness variability of the 2011 Tohoku-Oki tsunami deposits along the coastline of Sendai Bay. *Mar Geol* 358:38–48
- Goto T, Satake K, Sugai T, Ishibe T, Harada T, Gusman AR (2017) Effects of topography on particle composition of 2011 tsunami deposits on the ria-type Sanriku coast, Japan. *Quatern Int* 456:17–27. <https://doi.org/10.1016/j.quaint.2017.05.014>
- Gusman AR, Goto T, Satake K, Takahashi T, Ishibe T (2018) Sediment transport modeling of multiple grain sizes for the 2011 Tohoku tsunami on a steep coastal valley of Numanohama, Northeast Japan. *Mar Geol* 405:77–91
- Harada K, Aburaya T, Hamzah L, Imamura F (2000) Discussion about the effect of tide protecting forests to reduce tsunamis. *Proc Coast Eng JSCE* 47:366–370 (in Japanese)
- Ide S, Baltay A, Beroza GC (2011) Shallow dynamic overshoot and energetic deep rupture in the 2011 Mw 9.0 Tohoku-Oki earthquake. *Science* 332(6036):1426–1429
- Imai K, Harada K, Watanabe O, Esashi T, Shimanuki N, Yagi T, Imamura F (2009) Tsunami hazard mitigation by using coastal forest in a practical field—case study of Iwanuma-Natori Coast in Sendai Bay. *J Jpn Soc Civil Eng Ser B2 (coast Eng)* 65:326–330 (in Japanese with English abstract)
- Imai K, Horiuchi S, Imamura F (2013) Investigation on the dependence of tsunami trace heights distribution tsunami source presumption. *J Jpn Soc Civil Eng Ser B2 (Coast Eng)* 69(2):L_431–L_435 (in Japanese with English abstract)
- Kajiura K (1963) Leading wave of a tsunami. *Bull Earthquake Res Inst* 41:535–571
- Kusumoto S, Goto T, Sugai T, Omori T, Satake K (2018) Geological evidence of tsunamis in the past 3800 years at a coastal lowland in the Central Fukushima Prefecture, Japan. *Mar Geol* 404:137–146
- Kusumoto S, Imai K, Gusman AR, Satake K (2020) Reduction effect of tsunami sediment transport by a coastal forest: numerical simulation of the 2011 Tohoku tsunami on the Sendai Plain, Japan. *Sediment Geol* 407:105740. <https://doi.org/10.1016/j.sedgeo.2020.105740>
- Kusumoto S (2021) Reexamination of great earthquakes along the Japan trench based on geological analysis and numerical modeling for tsunami deposits. The University of Tokyo. <https://repository.dl.itc.u-tokyo.ac.jp/records/2001889>
- Mori N, Takahashi T, The 2011 Tohoku Earthquake Tsunami Joint Survey Group (2012) Nationwide post event survey and analysis of the 2011 Tohoku earthquake tsunami. *Coast Eng J* 54:1250001. <https://doi.org/10.1142/S0578563412500015>
- Okada Y (1985) Surface displacement due to shear and tensile faults in a half-space. *Bull Seismol Soc Am* 75(4):1135–1154
- Ozawa S, Nishimura T, Suito H, Kobayashi T, Tobita M, Imakiire T (2011) Coseismic and postseismic slip of the 2011 magnitude-9 Tohoku-Oki earthquake. *Nature* 475(7356):373–376
- Satake K, Fujii Y, Harada T, Namegaya Y (2013) Time and space distribution of coseismic slip of the 2011 Tohoku earthquake as inferred from tsunami waveform data. *Bull Seismol Soc Am* 103(2B):1473–1492
- Sugawara D, Yu NT, Yen JY (2019) Estimating a tsunami source by sediment transport modeling: a primary attempt on a historical/1867 normal-faulting tsunami in northern Taiwan. *J Geophys Res Earth Surf* 124:1675–1700
- Takahashi T, Shuto N, Imamura F, Asai D (1999) A movable bed model for tsunamis with exchange rate between bed load layer and suspended layer. *Proc Coast Eng* 46:606–610 (in Japanese)
- Takahashi T, Kurokawa T, Fujita M, Shimada H (2011) Hydraulic experiment on sediment transport due to tsunamis with various sand grain size. *J Jpn Soc Civil Eng Ser B2 (coast Eng)* 67:231–235
- Tanioka Y, Satake K (1996) Tsunami generation by horizontal displacement of ocean bottom. *Geophys Res Lett* 23(8):861–864
- Yamashita K, Sugawara D, Takahashi T, Imamura F, Saito Y, Imato Y, Kai T, Uehara H, Kato T, Nakata K, Saka R, Nishikawa A (2016) Numerical simulations of large-scale sediment transport caused by the 2011 Tohoku Earthquake Tsunami in Hirota Bay, Southern Sanriku Coast. *Coast Eng J* 58(4):1640015

Publisher's Note

Springer Nature remains neutral with regard to jurisdictional claims in published maps and institutional affiliations.

Submit your manuscript to a SpringerOpen® journal and benefit from:

- Convenient online submission
- Rigorous peer review
- Open access: articles freely available online
- High visibility within the field
- Retaining the copyright to your article

Submit your next manuscript at ► [springeropen.com](https://www.springeropen.com)